Indium Fluoroalkoxide Compounds

Liliana A. Mîinea, Seigi Suh, and David M. Hoffman*

Department of Chemistry and Materials Research Science and Engineering Center, University of Houston, Houston, Texas 77204

Received March 19, 1999

Reactions of indium amide complexes with fluorinated alcohols give indium fluoroalkoxide complexes. In[N-*t*-Bu($SiMe_3$)]$_3$ reacts with 3 equiv of $(CF_3)Me_2COH$ to give the homoleptic alkoxide dimer [In{μ-$OCMe_2(CF_3)$}{$OCMe_2(CF_3)$}$_2$]$_2$, but reactions involving the more acidic alcohols $(CF_3)_2MeCOH$ and $(CF_3)_2CHOH$ yield products containing *t*-$BuNH_2$, which is derived from the amide ligands. Thus, In[N-*t*-Bu($SiMe_3$)]$_3$ reacts with $(CF_3)_2$-MeCOH to give In[$OCMe(CF_3)_2$]$_3$(H_2N-*t*-Bu) and with $(CF_3)_2CHOH$ to yield In[$OCH(CF_3)_2$]$_3$(H_2N-*t*-Bu)$_3$ and [H_3N-*t*-Bu][In{$OCH(CF_3)_2$}$_4$(H_2N-*t*-Bu)]. Reactions of $(CF_3)_2MeCOH$ and $(CF_3)_2CHOH$ with In(tmp)$_3$ (tmp = the anion derived from 2,2,6,6-tetramethylpiperidine) and In(NEt_2)$_3$ are less complicated. In(tmp)$_3$ reacts with 3 equiv of $(CF_3)_2CHOH$ to give In[$OCH(CF_3)_2$]$_3$(Htmp) and with 4 equiv of $(CF_3)_2CHOH$ or $(CF_3)_2MeCOH$ to yield the salt compounds [H_2tmp][In{$OCR(CF_3)_2$}$_4$] (R = H, Me). Trigonal bipyramidal [H_2NEt_2][In{$OCH(CF_3)_2$}$_4$($HNEt_2$)] and octahedral *mer*-In[$OCMe(CF_3)_2$]$_3$(py)$_3$ are isolated from reactions involving In(NEt_2)$_3$. Crystal structure determinations of [In{μ-$OCMe_2(CF_3)$}{$OCMe_2(CF_3)$}$_2$]$_2$, [H_3N-*t*-Bu][In{$OCH(CF_3)_2$}$_4$(H_2N-*t*-Bu)]·EtOEt, In[$OCH(CF_3)_2$]$_3$(Htmp), [H_2tmp][In{$OCMe(CF_3)_2$}$_4$], In[$OCMe(CF_3)_2$]$_3$(py)$_3$, and [H_2NEt_2][In{$OCH(CF_3)_2$}$_4$-($HNEt_2$)] were carried out.

We recently reported the preparation of tin(II) and tin(IV) fluoroalkoxide complexes and the use of one of the compounds, Sn[$OCH(CF_3)_2$]$_4$($HNMe_2$)$_2$, to prepare transparent conductive fluorine-doped tin oxide films by chemical vapor deposition.[1,2] In the depositions, the fluorinated alkoxide ligands serve as an internal source of fluorine dopant, avoiding the need for a separate dopant source in the precursor mixture.[3]

The successful use of Sn[$OCH(CF_3)_2$]$_4$($HNMe_2$)$_2$ to prepare films prompted us to examine fluoroalkoxide complexes of other main group elements that can also form transparent conducting fluorine-doped oxides. In this report, we describe the synthesis of indium(III) fluoroalkoxide complexes, including several that are potential precursors to fluorine-doped indium oxide, an alternative to indium−tin oxide.[4−10] There appear to be no previously reported examples of indium(III) fluoroalkoxide complexes, but Roesky and co-workers have synthesized and structurally characterized the interesting indium(I) aryloxide dimer [In(μ-O-2,4,6-$(CF_3)_3C_6H_2$)]$_2$.[11] In addition, Mehrotra and co-workers have reported the synthesis of the nonfluorinated indium tris(alkoxide) compounds In(OR)$_3$ where R = Me, Et, *i*-Pr, *n*-Bu, *s*-Bu, *t*-Bu, and pentyl.[12]

Experimental Section

Synthesis. All manipulations were carried out in a glovebox or by using Schlenk techniques. The solvents were purified according to standard methods and then stored in the glovebox over molecular sieves. $InCl_3$ was used as received from Strem Chemicals Inc. In[N-*t*-Bu($SiMe_3$)]$_3$ and In(tmp)$_3$ (tmp = the anion derived from 2,2,6,6-tetramethylpiperidine) were synthesized as described in the literature,[13,14] and In(NEt_2)$_3$ was prepared in situ by a procedure derived from the published preparation.[15] $(CF_3)_2MeCOSiMe_3$ was identified in NMR spectra by comparison to an authentic sample (bp 65−67 °C) prepared by reacting Me_3SiNMe_2 with $(CF_3)_2MeCOH$. NMR spectra were collected on a 300-MHz instrument. Elemental analyses were performed by Oneida Research Services (Whitesboro, NY) and Chemisar Laboratories Inc. (Guelph, Ontario, Canada).

[In{μ-$OCMe_2(CF_3)$}{$OCMe_2(CF_3)$}$_2$]$_2$ (1). A hexane solution (8 mL) of $(CF_3)Me_2COH$ (0.56 g, 4.4 mmol) was added to a cold (−34 °C) solution of In[N-*t*-Bu($SiMe_3$)]$_3$ (0.79 g, 1.4 mmol) in hexane (50 mL). The reaction mixture was stirred for 18 h, and then the volatile components were distilled under vacuum, leaving a white solid. A mixture of hexane/CH_2Cl_2 (2:1) was added to the solid, and the resulting solution was filtered over Celite. The flask was transferred to a freezer (−34 °C), where the product formed as transparent crystals (yield 0.49 g, 68%). Anal. Calcd for $C_{24}H_{36}F_{18}In_2$: C, 29.03; H, 3.66. Found: C, 28.84; H, 3.52.

^{1}H NMR (C_6D_6): δ 1.5 (s, 12, μ-OC(CH_3)$_2$(CF_3)), 1.3 (s, 24, OC(CH_3)$_2$(CF_3)). ^{13}C{^{1}H} NMR (C_6D_6): δ 128 (q, 4, $^1J_{CF}$ = 285 Hz, OC(CH_3)$_2$(CF_3)), 127 (q, 2, $^1J_{CF}$ = 284 Hz, μ-OC(CH_3)$_2$(CF_3)), 77 (q, 2, $^2J_{CF}$ = 29 Hz, μ-O*C*(CH_3)$_2$(CF_3)), 75 (q, 4, $^2J_{CF}$ = 28 Hz, O*C*(CH_3)$_2$-(CF_3)), 27 (s, 8, OC(*C*H_3)$_2$(CF_3)), 24 (s, 4, μ-OC(*C*H_3)$_2$(CF_3)). IR (Nujol, KBr; cm^{-1}): 1323 m, 1284 w, 1196 s, 1151 vs, 1128 vs, 1043

(1) Suh, S.; Hoffman, D. M.; Atagi, L. M.; Smith, D. C.; Liu, J.-R.; Chu, W.-K. *Chem. Mater.* **1997**, *9*, 730.
(2) Suh, S.; Hoffman, D. M. *Inorg. Chem.* **1996**, *35*, 6164.
(3) Maruyama, T.; Tabata, K. *J. Appl. Phys.* **1990**, *68*, 4282.
(4) Avaritsiotis, J. N.; Howson, R. P. *Thin Solid Films* **1981**, *77*, 351.
(5) Avaritsiotis, J. N.; Howson, R. P. *Thin Solid Films* **1981**, *80*, 63.
(6) Singh, S. P.; Tiwari, L. M.; Agnihotri, O. P. *Thin Solid Films* **1986**, *139*, 1.
(7) Maruyama, T.; Nakai, T. *Jpn. J. Appl. Phys.* **1990**, *29*, L1705.
(8) Geoffroy, C.; Campet, G.; Portier, J.; Salardenne, J.; Couturier, G.; Bourrel, M.; Chabagno, J. M.; Ferry, D.; Quet, C. *Thin Solid Films* **1991**, *202*, 77.
(9) Maruyama, T.; Nakai, T. *J. Appl. Phys.* **1992**, *71*, 2915.
(10) Mirzapour, S.; Rozati, S. M.; Takwale, M. G.; Marathe, B. R.; Bhide, V. G. *J. Mater. Sci.* **1994**, *29*, 700.
(11) Scholz, M.; Noltemeyer, M.; Roesky, H. W. *Angew. Chem., Int. Ed. Engl.* **1989**, *28*, 1383.
(12) Chatterjee, S.; Bindal, S. R.; Mehrotra, R. C. *J. Indian Chem. Soc.* **1976**, *53*, 867.
(13) Kim, J.; Bott, S. G.; Hoffman, D. M. *Inorg. Chem.* **1998**, *37*, 3835.
(14) Frey, R.; Gupta, V. D.; Linti, G. *Z. Anorg. Allg. Chem.* **1996**, *622*, 1060.
(15) Rossetto, G.; Brianese, N.; Camporese, A.; Porchia, M.; Zanella, P.; Bertoncello, R. *Main Group Met. Chem.* **1991**, *14*, 113.

10.1021/ic990315j CCC: $18.00
Published on Web 09/08/1999

m, 1004 m, 970 m, 885 m, 873 m, 825 w, 758 m, 636 m, 597 w, 582 m, 545 w, 430 s, 414 s.

In[OCMe(CF$_3$)$_2$]$_3$(H$_2$N-*t*-Bu) (2). A toluene solution (8 mL) of (CF$_3$)$_2$MeCOH (1.0 g, 5.6 mmol) was added to a solution of In[N-*t*-Bu(SiMe$_3$)]$_3$ (0.75 g, 1.4 mmol) in toluene (30 mL). The reaction mixture was heated at 80−90 °C under an argon atmosphere for 20 h. The resulting mixture was allowed to cool to room temperature and then was concentrated in vacuo to ≈5 mL. Ether (1 mL) was added, and the flask was transferred to the freezer (−34 °C). The product separated as colorless crystals (yield 0.52 g, 52%). Anal. Calcd for $C_{16}H_{20}F_{18}NO_3In$: C, 26.28; H, 2.76; N, 1.91; F, 46.76. Found: C, 26.14; H, 2.58; N, 1.87; F, 46.57.

^{1}H NMR (C_6D_6): δ 2.2 (br, 2, N*H*), 1.5 (s, 9, OC(C*H*$_3$)(CF$_3$)$_2$), 0.58 (s, 9, C(C*H*$_3$)$_3$). ^{13}C{^{1}H} NMR (C_6D_6): δ 125 (q, 6, $^1J_{CF}$ = 288 Hz, OC(*C*F$_3$)$_2$(CH$_3$)), 78 (septet, 3, $^2J_{CF}$ = 29 Hz, O*C*(CF$_3$)$_2$(CH$_3$)), 54 (s, 1, H$_2$N*C*(CH$_3$)$_3$), 29 (s, 3, H$_2$NC(*C*H$_3$)$_3$), 20 (s, 3, OC(CF$_3$)$_2$(*C*H$_3$)). IR (Nujol, KBr; cm^{-1}): 3323 w and 3269 w [ν(N−H)], 1575 w, 1310 s, 1207 s, 1176 s, 1119 m, 1078 s,1026 w, 970 m, 864 m, 763 w, 702 m, 673 w, 621 w, 570 m.

In[OCH(CF$_3$)$_2$]$_3$(H$_2$N-*t*-Bu)$_3$ (3). A toluene solution (8 mL) of (CF$_3$)$_2$CHOH (1.4 g, 8.2 mmol) was added to a solution of In[N-*t*-Bu(SiMe$_3$)]$_3$ (0.75 g, 1.4 mmol) in toluene (30 mL). The reaction mixture was stirred for 20 h, resulting in a clear pale-yellow solution. The flask was moved to the freezer (−34 °C for 24 h), where transparent crystals separated. The crystals were filtered from the mother liquor, washed with cold toluene (10 mL), and then dried in vacuo, leaving the product as a white solid (yield 0.49 g, 43% based on In). Anal. Calcd for $C_{21}H_{36}F_{18}N_3O_3In$: C, 29.89; H, 4.02; N, 4.47. Found: C, 29.65; H, 3.97; N, 4.57.

^{1}H NMR (C_6D_6): δ 4.9 (septet, 3, $^3J_{CF}$ = 6.3 Hz, OC*H*(CF$_3$)$_2$), 2.2 (s, 6, *H*$_2$N-*t*-Bu), 0.91 (s, 18, H$_2$CN(C*H*$_3$)$_3$). ^{13}C{^{1}H} NMR (CD_2Cl_2): δ 124 (q, 6, $^1J_{CF}$ = 287 Hz, OCH(*C*F$_3$)$_2$), 73 (septet, 3, $^2J_{CF}$ = 31 Hz, O*C*H(CF$_3$)$_2$), 51 (s, 3, H$_2$N*C*(CH$_3$)$_3$), 31 (s, 9, H$_2$NC(*C*H$_3$)$_3$). IR (Nujol, KBr; cm^{-1}): 3335 m and 3283 w [ν(N−H)], 1574 m, 1280 s, 1257 s, 1203 s, 1172 s, 1143 w, 1087 m, 1022 m, 927 w, 881 m, 852 s, 742 m, 684 s.

[H$_3$N-*t*-Bu][In{OCH(CF$_3$)$_2$}$_4$(H$_2$N-*t*-Bu)] (4). Method A. The filtered mother liquor from the synthesis of **3** was concentrated to 7 mL. The flask was placed in the freezer (−34 °C), where colorless crystals separated (yield 0.2 g, 15% based on In in the procedure to prepare **3**).

Method B. A toluene solution (10 mL) of (CF$_3$)$_2$CHOH (1.4 g, 8.2 mmol) was added to a solution of In[N-*t*-Bu(SiMe$_3$)]$_3$ (0.50 g, 0.91 mmol) in toluene (40 mL). The reaction mixture was stirred for 18 h, resulting in a clear colorless solution. The solution was concentrated in vacuo to ≈5 mL, and 1 mL of ether was added. The flask was placed in the freezer, where a white solid separated. The mother liquor was removed with a pipet, and the remaining solid was dried under vacuum (yield 0.45 g, 53%). Anal. Calcd for $C_{20}H_{27}F_{24}N_2O_4In$: C, 25.82; H, 2.93; N, 3.01. Found: C, 25.96; H, 2.87; N, 3.01.

^{1}H NMR (C_6D_6): δ 5.1 (septet, 4, $^3J_{CF}$ = 6.3 Hz, OC*H*(CF$_3$)$_2$), 3.6 (br, 5, *H*$_2$N-*t*-Bu/*H*$_3$N-*t*-Bu), 0.8 (s, 18, H$_2$NC*Me*$_3$/H$_3$NC*Me*$_3$). ^{13}C{^{1}H} NMR (C_6D_6): δ 124 (q, 8, $^1J_{CF}$ = 285 Hz, OCH(*C*F$_3$)$_2$), 73 (septet, 4, $^2J_{CF}$ = 31 Hz, O*C*H(CF$_3$)$_2$), 51 (s, 2, H$_2$N*C*(CH$_3$)$_3$ and H$_3$N*C*(CH$_3$)$_3$), 29 (s, 6, H$_2$NC(*C*H$_3$)$_3$ and H$_3$NC(*C*H$_3$)$_3$). IR (Nujol, KBr; cm^{-1}): 3346 m, 3318 m, 3291 w and 3269 w [ν(*H*$_3$N-*t*-Bu)/*H*$_2$N-*t*-Bu)], 1633 m, 1602 w, 1574 s, 1518 vs, 1284 vs, 1257 vs, 1178 vs, 1125 vs, 1087 vs, 1024 s, 952 m, 887 vs, 854 vs, 796 m, 744 vs, 709 m, 672 s, 648 s, 522 s, 439 s.

In[OCH(CF$_3$)$_2$]$_3$(Htmp) (5). Method A. A toluene solution (10 mL) of (CF$_3$)$_2$CHOH (0.38 g, 2.3 mmol) was added slowly to a solution of In(tmp)$_3$ (0.41 g, 0.76 mmol) in toluene (25 mL) at −34 °C. After the solution was warmed to room temperature and stirred for 24 h, the volatile components were removed under vacuum from the pale yellow solution to give a yellow residue. Ether was added, and the mixture was filtered over Celite. The filtrate was collected in a flask, and 1 mL hexane was added to it. The flask was transferred to the freezer (−34 °C), and the product separated as yellow crystals (yield 0.39 g, 67%).

Method B. Solid In(tmp)$_3$ (0.072 g, 0.013 mmol) was added at room temperature to a toluene (15 mL) solution of **6** (0.37 g, 0.040 mmol). The flask was sealed and wrapped with aluminum foil to protect the mixture from light, and the solution was stirred for 19 h. The volatile components were removed in vacuo from the clear pale-yellow solution, leaving a yellow solid, which was pure product as judged by ^{1}H NMR. Anal. Calcd for $C_{18}H_{22}F_{18}NO_3In$: C, 28.55; H, 2.93; N, 1.84. Found: C, 28.06; H, 2.43; N, 1.76.

^{1}H NMR (C_6D_6): δ 4.8 (septet, 3, $^3J_{CF}$ = 5.4 Hz, OC*H*(CF$_3$)$_2$), 2.3 (br, 1, N*H*), 0.96 and 0.98 (2 × br s, 6 each, HN(C*Me*$_2$)$_2$(CH$_2$)$_2$CH$_2$), 0.85 (br q, 4, HN(CMe$_2$)$_2$(C*H*$_2$)$_2$CH$_2$), 0.28 (br pentet, 2, HN(CMe$_2$)$_2$-(CH$_2$)$_2$C*H*$_2$). ^{13}C{^{1}H} NMR (C_6D_6): δ 123 (q, 6, $^1J_{CF}$ = 285 Hz, OCH-(*C*F$_3$)$_2$), 73 (septet, 3, $^2J_{CF}$ = 32 Hz, O*C*H(CF$_3$)$_2$), 58 (s, 2, HN(*C*Me$_2$)$_2$-(CH$_2$)$_2$CH$_2$), 37 (s, 2, HN(CMe$_2$)$_2$(*C*H$_2$)$_2$CH$_2$), 33 and 24 (2 × s, 2 each, HN(C*Me*$_2$)$_2$(CH$_2$)$_2$CH$_2$), 16 (s, 1, HN(CMe$_2$)$_2$(CH$_2$)$_2$*C*H$_2$). IR (Nujol, KBr; cm^{-1}): 3215 w [ν(N−H)], 1604 w, 1290 s, 1269 s, 1215 s, 1188 s, 1142 s, 1095 s, 999 w, 976 w, 956 m, 893 s, 854 vs, 746 s, 686 vs.

[H$_2$tmp][In{OCH(CF$_3$)$_2$}$_4$] (6). Method A. A toluene solution (5 mL) of (CF$_3$)$_2$CHOH (0.25 g, 1.5 mmol) was added slowly to a cold (0 °C) solution of In(tmp)$_3$ (0.2 g, 0.4 mmol) in 20 mL of toluene. The reaction mixture was stirred for 16 h while the temperature was allowed to increase slowly to room temperature. The volatile components were removed in vacuo to give a yellowish white solid. The solid was dissolved in CH_2Cl_2 (5 mL), and the flask was transferred to the freezer (−34 °C). Transparent crystals separated (yield 0.25 g, 73%).

Method B. An excess of (CF$_3$)$_2$CHOH (0.23 g, 1.4 mmol) in toluene (5 mL) was added to a toluene (20 mL) solution of **5** (0.30 g, 0.39 mmol) at room temperature. After the reaction mixture was stirred for 23 h, the volatile components were removed under vacuum, leaving [H$_2$tmp][In(OCH(CF$_3$)$_2$)$_4$] as a white powder. Anal. Calcd for $C_{21}H_{24}F_{24}$-NO_4In: C, 27.50; H, 2.61; N, 1.50. Found: C, 27.28; H, 2.55; N, 1.48.

^{1}H NMR (C_6D_6): δ 5.9 (br t, 2, J_{NH} ≈ 45 Hz, N*H*), 4.7 (br septet, 4, $^3J_{CF}$ = 5.1 Hz, OC*H*(CF$_3$)$_2$), 0.84 (s, 12, H$_2$N(C*Me*$_2$)$_2$(CH$_2$)$_2$CH$_2$), 0.80 (s, 6, H$_2$N(CMe$_2$)$_2$(C*H*$_2$)$_2$C*H*$_2$). ^{13}C{^{1}H} NMR (C_6D_6): δ 123 (q, 8, $^1J_{CF}$ = 283 Hz, OCH(*C*F$_3$)$_2$), 73 (septet, 4, $^2J_{CF}$ = 32 Hz, O*C*H-(CF$_3$)$_2$), 58 (s, 2, H$_2$N(*C*Me$_2$)$_2$(CH$_2$)$_2$CH$_2$), 34 (s, 2, H$_2$N(CMe$_2$)$_2$(*C*H$_2$)$_2$-CH$_2$), 27 (s, 4, H$_2$N(C*Me*$_2$)$_2$(CH$_2$)$_2$CH$_2$), 15 (s, 1, H$_2$N(CMe$_2$)$_2$-(CH$_2$)$_2$*C*H$_2$). IR (Nujol, KBr; cm^{-1}): 3203 w and 3097 w [ν(N−H)], 1602 m, 1290 s, 1269 w, 1257 w, 1190 vs, 1120 m, 1099 m, 893 m, 856 s, 746 s, 686 s.

[H$_2$tmp][In(OCMe(CF$_3$)$_2$)$_4$] (7). A toluene solution (8 mL) of (CF$_3$)$_2$MeCOH (1.02 g, 5.6 mmol) was added to a solution of In(tmp)$_3$ (0.75 g, 1.4 mmol) in toluene (30 mL). The flask was sealed, wrapped in aluminum foil to shield the mixture from light, and then heated in an oil bath at 80−90 °C for 20 h (*caution*! closed flask heating). After the mixture was allowed to cool to room temperature, it was concentrated in vacuo to 5 mL. A white solid separated. The solid was filtered off, washed with toluene (10 mL), and dried (3 h) under vacuum (yield 0.25 g). Ether (1 mL) was added to the filtrate, and the flask was transferred to the freezer (−34 °C). A second crop of product separated as transparent crystals (0.32 g) (total yield 0.57 g, 42%). Anal. Calcd for $C_{25}H_{32}F_{24}NO_4In$: C, 30.60; H, 3.29; N, 1.42. Found: C, 30.14; H, 3.08; N, 1.58.

^{1}H NMR (C_6D_6): δ 5.5 (br t, 2, J_{HH} ≈ 45 Hz, N*H*), 1.75 (s, 9, OC-(C*H*$_3$)(CF$_3$)$_2$), 0.87 (s, 12, H$_2$N(C*Me*$_2$)$_2$(CH$_2$)$_2$CH$_2$), 0.81 (m, 2, H$_2$N-(CMe$_2$)$_2$(CH$_2$)$_2$C*H*$_2$), 0.80 (m, 4, H$_2$N(CMe$_2$)$_2$(C*H*$_2$)$_2$CH$_2$). ^{13}C{^{1}H} NMR (CD_2Cl_2): δ 124 (q, 8, $^1J_{CF}$ = 288 Hz, OC(*C*F$_3$)$_2$(CH$_3$)), 77 (septet, 4, $^2J_{CF}$ = 29 Hz, O*C*(CF$_3$)$_2$(CH$_3$)), 60 (s, 2, H$_2$N(*C*Me$_2$)$_2$(CH$_2$)$_2$-CH$_2$), 35 (s, 2, H$_2$N(CMe$_2$)$_2$(*C*H$_2$)$_2$CH$_2$), 27 (s, 4, H$_2$N(C*Me*$_2$)$_2$(CH$_2$)$_2$-CH$_2$), 20 (s, 4, OC(CF$_3$)$_2$(*C*H$_3$)), 16 (s, 1, H$_2$N(CMe$_2$)$_2$(CH$_2$)$_2$*C*H$_2$). IR (Nujol, KBr; cm^{-1}): 3186 m and 3109 m [ν(N−H)], 1587 s, 1554 w, 1307 vs, 1221 vs, 1182 vs, 1163 vs, 1120 s, 1078 m, 1008 m, 958 s, 895 w, 882 m, 763 m, 700 vs, 682 m, 628 s, 534 s, 430 m, 410 m.

In[OCMe(CF$_3$)$_2$]$_3$(py)$_3$ (8). Method A. An excess of pyridine (0.50 g, 6.3 mmol) in ether (3 mL) was added at room temperature to a solution of **2** (0.15 g, 0.21 mmol) in ether (10 mL). The reaction mixture was stirred for 12 h, and then the volatile components were removed in vacuo, leaving a yellowish white residue. Crystallization from an ether/hexanes solution at −34 °C gave the product as transparent, colorless crystals (yield 0.17 g, 91%).

Method B. A large excess of pyridine (0.25 g, 3.1 mmol) in hexane (3 mL) was added at room temperature to a suspension of **7** (0.11 g,

Table 1. Crystallographic Data for $[In\{\mu\text{-}OCMe_2(CF_3)\}\{OCMe_2(CF_3)\}_2]_2$ (**1**), $[H_3N\text{-}t\text{-}Bu][In\{OCH(CF_3)_2\}_4(H_2N\text{-}t\text{-}Bu)]\cdot EtOEt$ (**4**), $In[OCH(CF_3)_2]_3(Htmp)$ (**5**), $[H_2tmp][In\{OCMe(CF_3)_2\}_4]$ (**7**), $In[OCMe(CF_3)_2]_3(py)_3$ (**8**), and $[H_2NEt_2][In\{OCH(CF_3)_2\}_4(HNEt_2)]$ (**9**)

	1	**4**·EtOEt	**5**	**7**	**8**	**9**
formula	$C_{24}H_{36}F_{18}In_2O_6$	$[C_4H_{12}N]$-$[C_{16}H_{15}F_{24}InNO_4]$·-$C_4H_{10}O$	$C_{18}H_{22}F_{18}InNO_3$	$[C_9H_{20}N]$-$[C_{16}H_{12}F_{24}InO_4]$	$C_{27}H_{24}F_{18}InN_3O_3$	$[C_4H_{12}N]$-$[C_{16}H_{15}F_{24}InNO_4]$
fw	992.17	1004.38	757.19	981.34	895.31	930.31
crystal dimens mm	0.35 × 0.15 × 0.10	0.30 × 0.20 × 0.08	0.45 × 0.35 × 0.35	0.45 × 0.45 × 0.35	0.45 × 0.35 × 0.30	0.12 × 0.40 × 0.50
λ (Mo Kα), Å	0.710 73	0.710 73	0.710 73	0.710 73	0.710 73	0.710 73
space group	*C*2/*c* (monoclinic)	$P\bar{1}$ (triclinic)	$P2_1/n$ (monoclinic)	$P2_1/n$ (monoclinic)	$P\bar{1}$ (triclinic)	$P2_1/c$ (monoclinic)
a, Å	21.3967(13)	9.6785(6)	14.7601(10)	13.0022(8)	10.5373(6)	34.996(8)
b, Å	18.3406(11)	10.8725(6)	11.3221(8)	17.4119(11)	12.7022(7)	9.946(2)
c, Å	20.0887(13)	19.4295(11)	17.8837(12)	16.3536(10)	12.8076(7)	19.470(4)
α, deg		79.3940(10)			88.2640(10)	
β, deg	115.877(1)	89.8450(10)	112.8930(10)	99.1810(10)	88.2580(10)	95.44(2)
γ, deg		78.8460(10)			79.6350(10)	
T, °C	−50(2)	−50(2)	−50(2)	−50(2)	−50(2)	−75
Z	8	2	4	4	2	8
V, Å^3	7092.9(8)	1970.5(2)	2753.2(3)	3654.9(4)	1684.97(16)	6746
D_{calcd}, g/cm^3	1.858	1.693	1.827	1.783	1.765	1.83
μ, cm^{-1}	14.30	7.48	10.02	8.01	8.35	8.47
R, R_w	0.0560, 0.1384[a]	0.0301, 0.0784[b]	0.0208, 0.0513[c]	0.0213, 0.0523[d]	0.0281, 0.0746[e]	0.059, 0.051[f]

[a] $R = \sum||F_o| - |F_c||/\sum|F_o|$; $R_w = [\sum w(F_o^2 - F_c^2)^2/\sum w(F_o^2)^2]^{1/2}$, $w = [\sigma^2(F_o^2) + (0.0483P)^2 + (172.0616P)]^{-1}$ where $P = (F_o^2 + 2F_c^2)/3$. [b] $R = \sum||F_o| - |F_c||/\sum|F_o|$; $R_w = [\sum w(F_o^2 - F_c^2)^2/\sum w(F_o^2)^2]^{1/2}$, $w = [\sigma^2(F_o^2) + (0.0349P)^2 + (2.7091P)]^{-1}$ where $P = (F_o^2 + 2F_c^2)/3$. [c] $R = \sum||F_o| - |F_c||/\sum|F_o|$; $R_w = [\sum w(F_o^2 - F_c^2)^2/\sum w(F_o^2)^2]^{1/2}$, $w = [\sigma^2(F_o^2) + (0.0184P)^2 + (2.3223P)]^{-1}$ where $P = (F_o^2 + 2F_c^2)/3$. [d] $R = \sum||F_o| - |F_c||/\sum|F_o|$; $R_w = [\sum w(F_o^2 - F_c^2)^2/\sum w(F_o^2)^2]^{1/2}$, $w = [\sigma^2(F_o^2) + (0.0187P)^2 + (3.2449P)]^{-1}$ where $P = (F_o^2 + 2F_c^2)/3$. [e] $R = \sum||F_o| - |F_c||/\sum|F_o|$; $R_w = [\sum w(F_o^2 - F_c^2)^2/\sum w(F_o^2)^2]^{1/2}$, $w = [\sigma^2(F_o^2) + (0.0375P)^2 + (1.9749P)]^{-1}$ where $P = (F_o^2 + 2F_c^2)/3$. [f] $R = \sum||F_o| - |F_c||/\sum|F_o|$, $R_w = [\sum w(|F_o| - |F_c|)^2/\sum w|F_o|^2]^{1/2}$, $w = [\sigma(F)]^{-2}$.

0.11 mmol) in 10 mL of hexane. The reaction mixture was stirred for 12 h, during which a white precipitate formed. The volatile components were removed in vacuo, leaving **8** as a white solid.

Method C. $LiNEt_2$ (0.55 g, 7.0 mmol) was slowly added to a suspension of $InCl_3$ (0.55 g, 2.3 mmol) in ether (25 mL). The reaction mixture became yellowish-brown. After 18 h of stirring, the ether was removed under vacuum, leaving a sticky brown solid. The solid was extracted with hexane (3 × 10 mL), and the extracts were combined and filtered. Hexane was removed from the filtrate in vacuo, leaving a viscous brown liquid. Toluene (20 mL) was added to the residue, and $(CF_3)_2MeCOH$ (1.3 g, 7.1 mmol) in toluene (6 mL) was then added to this solution. The reaction mixture was heated in an oil bath at 80 °C for 16 h under an argon atmosphere. The mixture was allowed to cool to room temperature, and the volatile components were removed in vacuo, leaving a viscous dark orange liquid. The orange liquid was dissolved in a mixture of hexane (15 mL) and CH_2Cl_2 (5 mL). A large excess of pyridine was added to the solution, and the mixture was stirred for 1 h. During this time, the product formed as a white solid. The reaction mixture was concentrated to half of its initial volume, and the concentrate was filtered to separate the product. The solid was washed with cold hexane (10 mL) and then dried in vacuo (yield 0.58 g, 29% based on $InCl_3$). A satisfactory analysis was not obtained. Anal. Calcd for $C_{27}H_{24}F_{18}N_3O_3In$: C, 36.2; H, 2.71; N, 4.69. Found: C, 35.15; H,; 2.25; N, 5.47.

^{1}H NMR (C_6D_6): δ 8.8 (d, 6, *o*-py), 6.8 (t, 3, *p*-py), 6.5 (t, 6, *m*-py), 1.3 (s, 9, $OC(CH_3)(CF_3)_2$). IR (Nujol, KBr; cm^{-1}): 1609 s, 1298 vs, 1209 s, 1178 vs, 1109 m, 1076 s, 1041 m, 1014 w, 962 m, 852 w, 758 m, 700 vs, 636 w, 615 w.

$[H_2NEt_2][In\{OCH(CF_3)_2\}_4(HNEt_2)]$ (9). $LiNEt_2$ (2.1 g, 27 mmol) was slowly added to a suspension of $InCl_3$ (2.0 g, 8.8 mmol) in ether (15 mL). The reaction mixture became yellowish-brown. After 18 h of stirring, the ether was removed under vacuum to give a sticky brown solid. The solid was extracted with hexane (3 × 10 mL), and the extracts were combined and filtered. The volume of the light brown filtrate was reduced in vacuo to ca. 7 mL. The solution was cooled to −30 °C, and $(CF_3)_2CHOH$ (4.1 g, 24 mmol) was added slowly to the cold solution over a period of 20 min. After the addition was complete, the reaction mixture was allowed to warm to room temperature and was stirred for an additional 2 h. The volatile components were then removed in vacuo to give a sticky brown solid. The product was sublimed (85−95 °C/0.06 mmHg) from the solid as a white powder (yield 4.30 g, 53% based on In). The product could also be crystallized from ether/dichloromethane (3:1) at −35 °C. A satisfactory carbon analysis was not obtained. Anal. Calcd for $C_{20}H_{27}F_{24}N_2O_4In$: C, 25.82; H, 2.93; N, 3.01. Found: C, 24 81; H, 2.50; N, 2.64.

^{1}H NMR ($CDCl_3$): δ 8.1 (br, 3, $HN(CH_2CH_3)$ and $H_2N(CH_2CH_3)$), 4.84 (br septet, 4, $^3J_{CF}$ = 6.3 Hz, $OCH(CF_3)_2$), 2.98 (br q, 8, $N(CH_2CH_3)_2$), 1.26 (t, 12, $N(CH_2CH_3)_2$). ^{13}C{^{1}H} NMR (C_6D_6): δ 124 (q, 8, $^1J_{CF}$ = 287 Hz, $OCH(CF_3)_2$), 74 (septet, 4, $^2J_{CF}$ = 31 Hz, $OCH(CF_3)_2$), 43.3 (s, 4, $N(CH_2CH_3)_2$), 13.2 (s, 4, $N(CH_2CH_3)_2$). IR (Nujol, CsI; cm^{-1}): 3290 w and 3161 w [ν(N−H)], 1282 s, 1255 s, 1209 s, 1182 s, 1191 s, 887 m, 855 s, 745 m, 687 m, 523 m.

X-ray Crystallography. Crystal data are presented in Table 1. The crystals are colorless blocks (**1**, **5**), flat columns (**4**·EtOEt), prismatic blocks (**7**), parallelepipeds (**8**), and plates (**9**). The crystals were manipulated under mineral oil during the mounting procedures. Crystals for analyses were grown at low temperature (−34 °C) from saturated hexane/ether (**1**), toluene/ether (**4**·EtOEt), ether (**5**, **7**, **8**), and CH_2Cl_2 (**9**) solutions. In the case of **9**, a sublimed sample was used for the crystallization.

Measurements for crystals of **1**, **4**·EtOEt, **5**, **7**, and **8** were made with a Siemens SMART platform diffractometer equipped with a 1K CCD area detector. A hemisphere of data (1271 frames at 5 cm detector distance) was collected using a narrow-frame method with scan widths of 0.30% in ω and an exposure time of 20 s/frame. The first 50 frames were remeasured at the end of data collection to monitor instrument and crystal stability, and the maximum correction on *I* was <1%. The data were integrated using the Siemens SAINT program, with the intensities corrected for the Lorentz factor, polarization, air absorption, and absorption due to variation in the path length through the detector faceplate. A ψ-scan absorption correction was applied on the basis of the entire data set. Redundant reflections were averaged. The asymmetric unit of **1** consists of two half-molecules situated about 2-fold axes. Several of the alkoxide ligands are heavily disordered, and this was treated by a combination of ideal rigid body groups and constraints on distances and thermal parameters. The ether solvent molecule in **4** was found to be disordered over two positions having approximate populations of 70%:30%. Distance constraints were used within the disordered moieties. The ammonium hydrogens in **7** were refined independently. Calculations for **1**, **4**·EtOEt, **5**, **7**, and **8** were performed using SHELXS-97.

The crystal of **9** was mounted in a random orientation on the Nicolet R3m/V automatic diffractometer. The sample was placed in a stream of dry nitrogen gas at −75 °C (previous experiments had shown the

Scheme 1

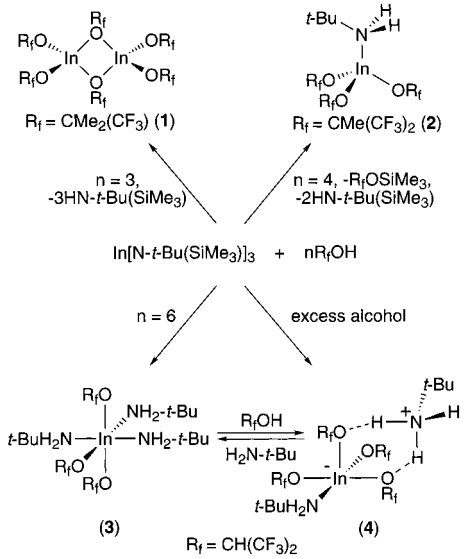

material to be unstable at −50 °C). Intensities were measured using the ω-scan technique. Two standard reflections were monitored after every 2 h or every 100 data collected, and these showed a 10% linear decay over the course of the experiment. A normalization factor as a function of X-ray exposure time was applied to account for this. During data reduction, Lorentz and polarization corrections were applied, as well as a semiempirical absorption correction based on 10 reflections having χ values between 70 and 90°.

The structure was solved by interpretation of the Patterson map, which revealed the positions of the In atoms in the asymmetric unit consisting of two independent cation/anion pairs. Remaining non-hydrogen atoms were located in subsequent difference Fourier syntheses. The usual sequence of isotropic and anisotropic refinement was followed. Several areas in both independent molecules were found to be significantly disordered, and in each case, the final occupancy factors were determined by analysis of the isotropic thermal motion of the related atoms. Three of the alkoxide groups are disordered, and these were modeled as individual rigid bodies on the basis of the best fit found when each of the separate CF_3 groups was allowed to move independently. The final occupancy factors were 45%/55% for C1/C1′, 55%/45% for C27/C27′, and 50%/50% for the C30/C30′ groups. Two of the ethyl groups are also heavily disordered. The C15/C15′ locations were refined independently using 35%/65% occupancies, and the C39−C40/C39′−C40′ units were refined using mild distance constraints and 35%/65% occupancies. Hydrogens on the nondisordered alkoxide groups were positioned at ideal locations and constrained to riding motion. No unusually high correlations were noted between any of the variables in the last cycle of full-matrix least-squares refinement, and the final difference density map showed a maximum peak of about 0.9 e/A^3. Calculations were made using Nicolet's SHELXTL PLUS (1987) series of crystallographic programs.

Results and Discussion

Synthesis. Indium fluoroalkoxide complexes were prepared by reacting the indium amide complexes In[N-*t*-Bu(SiMe$_3$)]$_3$,[13] In(tmp)$_3$ (tmp = the anion derived from 2,2,6,6-tetramethylpiperidine),[14] and In(NEt$_2$)$_3$ (prepared in situ)[15] with (CF$_3$)Me$_2$COH, (CF$_3$)$_2$MeCOH, and (CF$_3$)$_2$CHOH. Schemes 1 and 2 summarize the synthetic results. It is noteworthy that, with the same alcohols and under similar reaction conditions, the hexamethyldisilazide complex In[N(SiMe$_3$)$_2$]$_3$ either did not react or reacted only partially with formation of multiple products.

In[N-*t*-Bu(SiMe$_3$)]$_3$ reacts with (CF$_3$)Me$_2$COH to give the dimer [In{μ-OCMe$_2$(CF$_3$)}{OCMe$_2$(CF$_3$)}$_2$]$_2$ (**1**) and amine. The dimer is a volatile solid (subliming at 100 °C, 0.05 mmHg)

Scheme 2

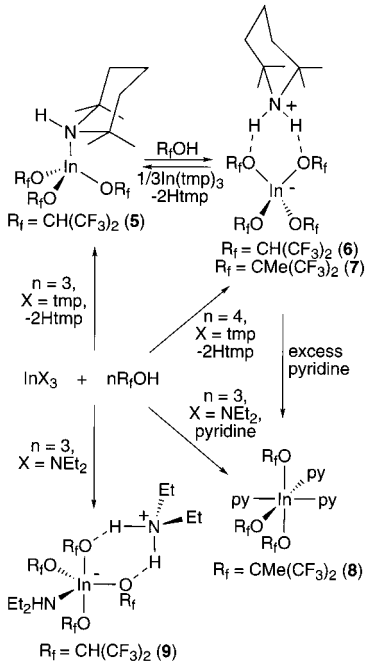

that is most conveniently isolated by crystallization from hexane/CH_2Cl_2. The ^{1}H NMR spectrum has two singlets in a 2:1 ratio, consistent with the dimer formulation and solid-state structure (see below). The formation of a homoleptic alkoxide dimer from the reaction of In[N-*t*-Bu(SiMe$_3$)]$_3$ with (CF$_3$)Me$_2$COH parallels the results of an analogous reaction involving *t*-BuOH, which produces [In(μ-OCMe$_3$)(OCMe$_3$)$_2$]$_2$.[16] In small-scale test reactions, compound **1** reacts quantitatively (as judged by ^{1}H NMR) with pyridine to form In[OCMe$_2$(CF$_3$)]$_3$(py)$_n$ (n = 1 or 2) with the value of n depending on the reaction stoichiometry.

In contrast to the reaction between In[N-*t*-Bu(SiMe$_3$)]$_3$ and (CF$_3$)Me$_2$COH to form **1**, the more acidic alcohols (CF$_3$)$_2$MeCOH and (CF$_3$)$_2$CHOH react with In[N-*t*-Bu(SiMe$_3$)]$_3$ to yield products that contain *t*-BuNH$_2$. Thus, In[N-*t*-Bu(SiMe$_3$)]$_3$ reacts with 4 equiv of (CF$_3$)$_2$MeCOH in hot toluene (80−90 °C) to give (CF$_3$)$_2$MeCOSiMe$_3$, Me$_3$Si(*t*-Bu)NH, and the amine adduct In[OCMe(CF$_3$)$_2$]$_3$(H$_2$N-*t*-Bu) (**2**). Compound **2** melts around 40 °C and sublimes at 60−68 °C/0.05 mmHg. When **2** is reacted with 1 or 2 equiv of the powerful donor ligand 4-(dimethylamino)pyridine, it takes up the extra amine to give five- and six-coordinate adducts that retain *t*-BuNH$_2$ (as indicated by NMR spectroscopy). *t*-BuNH$_2$ is fully displaced from **2**, yielding the tris(pyridine) adducts, only when reactions are carried out using 3 equiv of 4-(dimethylamino)pyridine or a large excess of unsubstituted pyridine.

The reaction between In[N-*t*-Bu(SiMe$_3$)]$_3$ and (CF$_3$)$_2$MeCOH is more complicated when it is carried out under mild conditions. At room or lower reaction temperatures (−78, −34, and 0 °C) and using 4 or 4.5 equiv of alcohol, a mixture of **2** and the salt [H$_2$N-*t*-Bu(SiMe$_3$)][In{OCMe(CF$_3$)$_2$}$_4$] is obtained, and when only 3 equiv of alcohol is used, starting material is observed in the product mix. Similarly, when 4 equiv of alcohol is reacted with In[N-*t*-Bu(SiMe$_3$)]$_3$ in an NMR tube (benzene-d_6; C$_6$Me$_6$ internal standard) at room temperature, an initial product distribution is observed consisting of **2** and [H$_2$N-*t*-Bu(SiMe$_3$)]-

(16) Suh, S.; Hoffman, D. M. *Abstracts of Papers*, 215th National Meeting of the American Chemical Society, Dallas, TX; American Chemical Society: Washington, DC, 1998; INOR 281. Suh, S.; Hoffman, D. M. Unpublished results.

$[In\{OCMe(CF_3)_2\}_4]$ in a 1:7 ratio, respectively, as well as $(CF_3)_2MeCOSiMe_3$ and $Me_3Si(t\text{-}Bu)NH$. After 16 h at room temperature, the ratio of **2** to $[H_2N\text{-}t\text{-}Bu(SiMe_3)][In\{OCMe(CF_3)_2\}_4]$ decreases to about 1:3. In large-scale reactions, $[H_2N\text{-}t\text{-}Bu(SiMe_3)][In\{OCMe(CF_3)_2\}_4]$ can be separated from **2** with difficulty and in low yield by repeated recrystallization from toluene or ether solutions. Heating (100−110 °C) a toluene solution of $[H_2N\text{-}t\text{-}Bu(SiMe_3)][In\{OCMe(CF_3)_2\}_4]$ for 22 h produces **2** cleanly, and heating a solid sample at the same temperature under dynamic vacuum also gives **2**, but there is some insoluble residue. These results indicate that $[H_2N\text{-}t\text{-}Bu(SiMe_3)][In\{OCMe(CF_3)_2\}_4]$ can be a precursor to **2** in the reaction between $In[N\text{-}t\text{-}Bu(SiMe_3)]_3$ and $(CF_3)_2MeCOH$. A complication, however, is that $(CF_3)_2MeCOH$ reacts with $Me_3Si(t\text{-}Bu)NH$ without the presence of any indium compound to form $(CF_3)_2MeCOSiMe_3$ and $t\text{-}BuNH_2$, presumably through a small concentration of a $[H_2N\text{-}t\text{-}Bu(SiMe_3)][OCMe(CF_3)_2]$ intermediate (eq 1). Thus, it is conceivable that **2** can also be

$$Me_3Si(t\text{-}Bu)NH + (CF_3)_2MeCOH \rightleftharpoons [H_2N\text{-}t\text{-}Bu(SiMe_3)][OCMe(CF_3)_2] \longrightarrow t\text{-}BuNH_2 + (CF_3)_2MeCOSiMe_3 \quad (1)$$

formed by an independent pathway involving "$In[OCMe(CF_3)_2]_3$" or its dimer reacting with free $t\text{-}BuNH_2$.

Another example illustrating the formation of $t\text{-}BuNH_2$ in reactions between $In[N(t\text{-}Bu)SiMe_3]_3$ and alcohol involves $(CF_3)_2CHOH$. $In[N(t\text{-}Bu)SiMe_3]_3$ reacts with 6 equiv of $(CF_3)_2CHOH$ in toluene to give the amine adduct $In[OCH(CF_3)_2]_3(H_2N\text{-}t\text{-}Bu)_3$ (**3**) in 43% isolated yield. Crystallization from the mother liquor produces the salt $[H_3N\text{-}t\text{-}Bu][In\{OCH(CF_3)_2\}_4(H_2N\text{-}t\text{-}Bu)]$ (**4**) in low yield. Compound **4** is prepared more conveniently in higher yield (53%) by reacting excess alcohol with the amide complex. Compounds **3** and **4** can be interconverted; compound **3** reacts with $(CF_3)_2CHOH$ to give **4**, and conversely, **4** reacts with excess $t\text{-}BuNH_2$ to give **3**.

The structure of **3** shown in Scheme 1 is based on the X-ray structure of the analogous compound $In[OCMe(CF_3)_2]_3(py)_3$ (see below). The structure of **4** was determined by X-ray crystallography. Room-temperature ^1H and ^{13}C NMR spectra of **3** and **4** show only one alkoxide ligand environment, suggesting both are fluxional. Similarly, the spectra show only one type of amine in **3** and the amine and ammonium ion in **4** give rise to averaged resonances. For **3**, low-temperature ^1H NMR spectra (CD_2Cl_2; to −40 °C) were generally uninformative, showing only some broadening of the resonances compared to those of the room-temperature spectrum. Bands are observed in IR spectra of **3** and **4** at around 3300 cm^{-1} that can be assigned to N−H stretches. As expected, the IR spectrum of **4** shows more bands in the N−H region than the IR spectrum of **3**.

The complications arising from the use of $In[N(t\text{-}Bu)SiMe_3]_3$ as a starting material prompted us to examine other types of amide complexes as precursors to alkoxide complexes (Scheme 2). The reaction of $In(tmp)_3$ with 3 and 4 equiv of $(CF_3)_2CHOH$ gives $In[OCH(CF_3)_2]_3(Htmp)$ (**5**) and $[H_2tmp][In\{OCH(CF_3)_2\}_4]$ (**6**), respectively. Similarly, the reaction with 4 equiv of $(CF_3)_2MeCOH$ gives $[H_2tmp][In\{OCMe(CF_3)_2\}_4]$ (**7**). Piperidine is expected to deprotonate $(CF_3)_2CHOH$ ($pK_a = 9.3$ vs ≈10.7 for $[tmpH_2]^+$) to some extent in toluene solution. This process could provide the source of ammonium alkoxide in the formation of **6** and **7**, or it is possible that the deprotonation is assisted by the coordination of the alcohol to indium, which would be expected to make the alcohol more acidic.

Compound **5** can be converted cleanly to **6** by reacting **5** with excess alcohol in toluene at room temperature. Conversely, heating **6** under vacuum (≈45 °C, 12 h) does not convert **6** to **5**, but the reaction of **6** with $In(tmp)_3$ in a 3:1 stoichiometry, respectively, gives **5**.

The structures of **5** and **7** shown in Scheme 2 are assigned on the basis of their respective X-ray crystal structures, and the structure of **6** is assumed by analogy to **7**. In the solid state, the piperidine-derived fragments in **5** and **7** have chair conformations. NMR spectra of **6** and **7** show only one sharp peak for the methyl groups, suggesting rapid chair−boat interconversion. In contrast, spectra for **5** have resonances arising from two different methyl groups. This indicates the piperidine ligand remains attached to the $In(OR_f)_3$ fragment; if the piperidine were coming on and off rapidly, umbrella-like inversion at the amine nitrogen coupled with chair−boat interconversion, both of which should be low-energy processes, would have rendered the methyl groups equivalent. There is one N−H band (3215 cm^{-1}) in the IR spectrum of **5** and two N−H bands(≈3200 and 3100 cm^{-1}) in the spectra of **6** and **7**, as expected.

Excess pyridine reacts with **2** or **7** to give $In[OCMe(CF_3)_2]_3(py)_3$ (**8**) quantitatively by ^1H NMR and in large-scale reactions in ≈90% isolated yields. Alternatively, **8** can be synthesized in low yield by reacting $In(NEt_2)_3$, prepared in situ from $InCl_3$ and $LiNEt_2$, with alcohol in hot toluene and then reacting the crude product from this reaction with excess pyridine. For the latter synthesis, the ^1H NMR spectrum of the crude product before the addition of pyridine suggests it is a mixture of two or more compounds. An analogous reaction between $In(NEt_2)_3$ and $HOCH(CF_3)_2$ carried out at room temperature produces the salt $[H_2NEt_2][In\{OCH(CF_3)_2\}_4(HNEt_2)]$ (**9**), which is readily isolated by vacuum sublimation.

The structure of **8** shown in Scheme 2 is assigned on the basis of its solid-state structure. The room-temperature ^1H NMR spectrum of **8** (benzene-d_6) shows resonances arising from only one type of alkoxide ligand and one type of pyridine ligand, which is inconsistent with the *mer*-octahedral structure observed in the solid state. At −80 °C, however, an apparent low-temperature limiting ^1H NMR spectrum is obtained (toluene-d_8) that shows resonances for the alkoxide and pyridine ligands in the expected 2:1 ratio. It was initially thought that the dynamic process to account for the temperature-dependent NMR might involve dissociation of pyridine to give a 5-coordinate intermediate, but the spectrum of **8** in neat pyridine-d_5 at −35 °C showed only one resonance for the alkoxide ligands. This points to a nondissociative fluxional process such as a Bailar twist mechanism. It is also possible that the molecule adopts a *fac* geometry in solution and that the apparent low-temperature limiting spectrum is actually the result of freezing out pyridine ligand rotation about the In−N bond.

X-ray Crystallographic Studies. X-ray crystallographic studies on **1** (Figure 1), **4** (Figure 2), **5** (Figure 3), **7** (Figure 4), **8** (Figure 5), and **9** (Figure 6) were carried out. Crystals of **1** and **9**, respectively, have two independent half-molecules and two independent cation/anion pairs in the asymmetric units. In both cases, several areas in the molecules were found to be significantly disordered, which was detrimental to the overall quality of the results.

Indium is four-coordinate in **1**, **5**, and **7**, five-coordinate in **4** and **9**, and six-coordinate in **8**. In the dimer **1**, the alkyl substituents on the four-membered $In(\mu\text{-}O)_2In$ ring have a syn configuration, and the ring itself has a slight butterfly configuration with a fold angle of 10.6° along the O1···O1′ vector (13.6° along In1···In1′). Compound **8** has a *mer*-octahedral

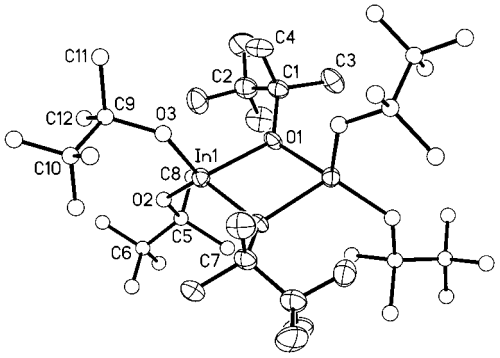

Figure 1. View of $[In\{\mu\text{-}OCMe_2(CF_3)\}\{OCMe_2(CF_3)\}_2]_2$ (**1**) (molecule 1) showing the atom-numbering scheme. Thermal ellipsoids are 40% equiprobability envelopes, with hydrogens omitted. Only one orientation of each disordered ligand is shown at any site.

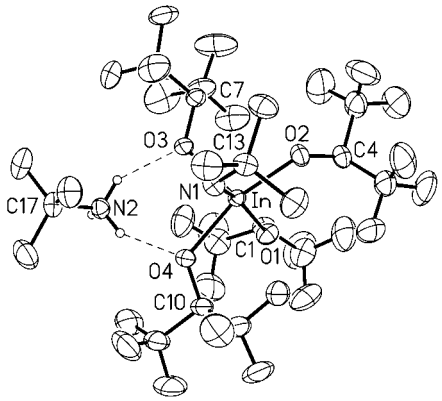

Figure 2. View of $[H_3N\text{-}t\text{-}Bu][In\{OCH(CF_3)_2\}_4(H_2N\text{-}t\text{-}Bu)]$ (**4**) showing the atom-numbering scheme. Thermal ellipsoids are 40% equiprobability envelopes. Hydrogen bonds are indicated by dashed lines.

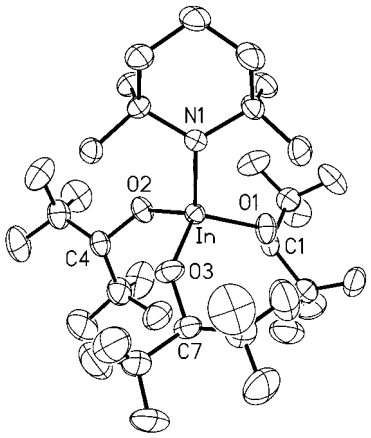

Figure 3. View of the $In[OCH(CF_3)_2]_3(Htmp)$ (**5**) molecule showing the atom-numbering scheme. Thermal ellipsoids are 40% equiprobability envelopes.

geometry with internal angles ranging from 80 to 99° and from 163 to 178° (see Table 2).

Compound **4** is best described as square pyramidal, where O3 occupies the apical position. The O3−In−O and O3−In−N1 angles range from 90 to 113°. O3 and O4 are involved in hydrogen bonding with the cation $[t\text{-}BuNH_3]^+$, which also interacts with diethyl ether in the lattice ($N\cdots OEt_2 = 2.86$ Å). Compound **9**, in contrast, is trigonal bipyramidal with the apical positions occupied by O1 and O2. The O1−In−O2 angle is 172°, and the angles in the trigonal plane sum to 359°. O2 and O3 are hydrogen-bonded to the cation $[H_2NEt_2]^+$.

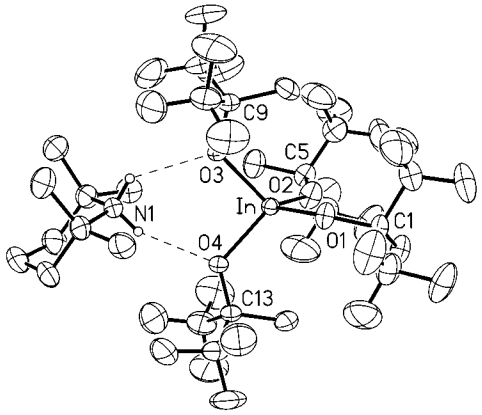

Figure 4. View of $[H_2tmp][In\{OCMe(CF_3)_2\}_4]$ (**7**) showing the atom-numbering scheme. Thermal ellipsoids are 40% equiprobability envelopes. Hydrogen bonds are indicated by dashed lines.

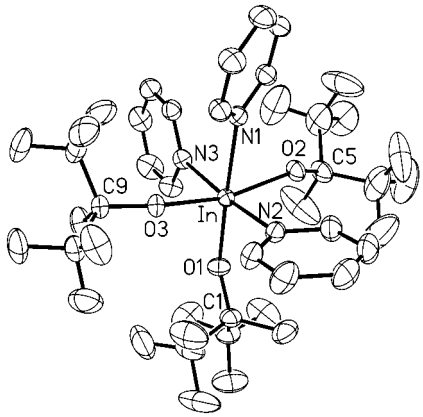

Figure 5. View of the $In[OCMe(CF_3)_2]_3(py)_3$ (**8**) molecule showing the atom-numbering scheme. Thermal ellipsoids are 40% equiprobability envelopes.

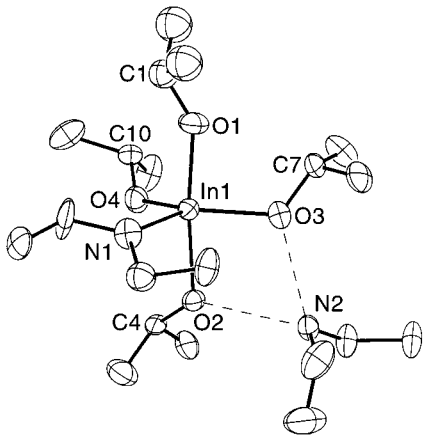

Figure 6. View of $[H_2NEt_2][In\{OCH(CF_3)_2\}_4(HNEt_2)]$ (**9**) (cation−anion pair 1) showing the atom-numbering scheme. Thermal ellipsoids are 35% equiprobability envelopes, with hydrogens and fluorines omitted. Only one orientation of each disordered group is shown.

Compounds **5** and **7** have distorted tetrahedral geometries. In **7**, the angles around In range from 95 to 121° with the smallest angle between O3 and O4, the result of hydrogen bonding with the cation $[H_2tmp]^+$. In **5**, the angles around In range from 95 to 116°. In this case, the smallest angle is O3−In−N1. Of the three alkoxide ligands, the O3 alkoxide is the least crowded by the piperidine methyl groups, which may account for the smaller angle. The piperidine in **5** and the piperidinium ion in **7** have chair conformations.

Table 2. Selected Bond Distances (Å) and Angles (deg) for $[In\{\mu\text{-}OCMe_2(CF_3)\}\{OCMe_2(CF_3)\}_2]_2$ (**1**), $[H_3N\text{-}t\text{-}Bu][In\{OCH(CF_3)_2\}_4(H_2N\text{-}t\text{-}Bu)]$ (**4**), $In[OCH(CF_3)_2]_3(Htmp)$ (**5**), $[H_2tmp][In\{OCMe(CF_3)_2\}_4]$ (**7**), $In[OCMe(CF_3)_2]_3(py)_3$ (**8**), and $[H_2NEt_2][In\{OCH(CF_3)_2\}_4(HNEt_2)]$ (**9**)

	1[a]	**4**	**5**	**7**	**8**	**9**[f]
In−O1	2.129(5)	2.071(3)	2.0043(16)	2.0060(16)	2.0891(18)	2.102(9)
In−O2	1.94(2)[b]	2.042(3)	2.0186(16)	2.0108(17)	2.1237(18)	2.164(8)
In−O3	1.970(9)[b]	2.089(2)	2.0118(17)	2.0470(15)	2.1097(17)	2.113(9)
In−X	2.134(5) (X = O1′)	2.117(2) (X = O4)	2.2004(19) (X = N1)	2.0539(15) (X = O4)	2.379(2) (X = N1)	2.075(8) (X = O4)
In−Y		2.308(3) (Y = N1)			2.296(2) (Y = N2)	2.253(11) (Y = N1)
In−Z					2.303(2) (Z = N3)	
N···O		2.841(4), 2.892(4)		3.065(3), 3.149(3)		2.75, 2.73
O1−In−O2	114.8(9), 127.6(2)[c]	93.61(11)	104.94(7)	103.71(7)	98.85(8)	172.4(3)
O1−In−O3	104.5(6)−113.9(5)[d]	113.07(11)	115.90(8)	107.90(7)	98.25(8)	88.5(4)
O1−In−X	75.8(2) (X = O1′)	89.91(11) (X = O4)	114.43(7) (X = N1)	115.45(7) (X = O4)	177.70(7) (X = N1)	99.7(4) (X = O4)
O1−In−Y		156.04(12) (Y = N1)			97.75(8) (Y = N2)	92.8(4) (Y = N1)
O1−In−Z					87.74(8) (Z = N3)	
O2−In−O3	113.7(5)−120.0(9)[d]	103.72(10)	110.67(8)	121.23(7)	162.79(7)	84.8(3)
O2−In−X	116.2(2), 126.8(9)[c] (X = O1′)	157.09(11) (X = O4)	116.03(7) (X = N1)	113.82(8) (X = O4)	80.23(8) (X = N1)	87.4(3) (X = O4)
O2−In−Y		88.00(11) (Y = N1)			89.55(8) (Y = N2)	87.7(3) (Y = N1)
O2−In−Z					88.72(8) (Z = N3)	
O3−In−X	99.4(5)−107.2(8)[d] (X = O1′)	95.63(10) (X = O4)	95.15(7) (X = N1)	95.21(6) (X= O4)	82.61(7) (X = N1)	130.8(3) (X = O4)
O3−In−Y		89.63(11) (Y = N1)			86.23(7) (Y = N2)	121.7(4) (Y = N1)
O3−In−Z					93.89(7) (Z = N3)	
X−In−Y		79.88(11) (X = O4, Y = N1)			80.16(8) (X = N1, Y = N2)	106.4(4) (X = O4, Y = N1)
X−In−Z					94.34(8) (X = N1, Z = N3)	
Y−In−Z					174.44(8) (Y = N2, Z = N3)	
avg $In-O_t-C$		125.1(2)	126.52(16)	131.90(16)	142.80(19)	134.32(8)
range		119.2(2)−133.3(2)	123.49(25)− 130.46(16)	124.91(15)− 139.42(16)	142.09(16)− 143.80(19)	122.0(8)−150.2(8)
In−O−In′	103.5(2)					

[a] Distances and angles for only one of the two independent half-molecules in the asymmetric unit are presented. Full details can be found in the Supporting Information. [b] The average distance for the different orientations in the disordered model. [c] The angles for the two different orientations in the disordered model. [d] The range of angles for the different orientations in the disordered model. [e] Distances and angles for only one of the two independent cation−anion pairs in the asymmetric unit are presented.

The $In-O_{terminal}$ distances in the six compounds range from 1.94(2) to 2.164(8) Å. In **8**, the In−O distance to the alkoxide trans to pyridine is slightly shorter than the distances to the mutually trans alkoxides. This reflects the greater trans influence of the alkoxide compared to pyridine. In the compounds where there is hydrogen bonding between cations and alkoxide oxygen atoms, the corresponding In−O distances are lengthened slightly by the interaction. The cluster $In_5(\mu_5\text{-}O)(\mu_3\text{-}O\text{-}i\text{-}Pr)_4(\mu_2\text{-}O\text{-}i\text{-}Pr)_4(O\text{-}i\text{-}Pr)_5$ is the only other structurally characterized indium complex with terminal In−OR bonds, and in it, the distances are 1.957(15)−1.988(16) Å, which are close to the short end of the range we observe.[17,18] The $In-O_{bridge}$ bond distances in **1** [2.129(5) and 2.134(5) Å] are similar to the distances reported for the $In_2(\mu\text{-}OR)_2$ cores in alkylindium alkoxide dimers: $[t\text{-}Bu_2In(\mu\text{-}OMe)]_2$ [average 2.153(2) Å],[19] $[t\text{-}Bu_2In(\mu\text{-}OEt)]_2$ [average 2.156(5) Å],[20] $[Ph_2In(\mu\text{-}OSiMe_3)]_2$ [average 2.154(8) Å],[21] and $[(Me_3SiCH_2)_2In(\mu\text{-}OSiMe_3)]_2$ [average 2.163(7) Å].[22] The $In-O_{bridge}$ distances in $[In(\mu\text{-}OC_2H_5)(SC_5H_4N)_2]_2$, a dimer with octahedral In atoms, average 2.132(3) Å.[23] Interestingly, the distances in the indium(I) dimer $[In(\mu\text{-}O\text{-}2,4,6\text{-}(CF_3)_3C_6H_2)]_2$ (average 2.320 Å),[11] which has an empty p orbital on each In atom available for π interaction, are significantly longer than those in the indium(III) compounds, the opposite of what might have been expected.

The In−N bond distances in **4**, **5**, **8**, and **9** range from 2.2004(19) to 2.379(2) Å. The In−N distance in tetrahedral **5** is the shortest, while the longest is to the pyridine trans (N1) to the alkoxide ligand in octahedral **8**. In **8**, the In−N distances to the mutually trans pyridine ligands are 0.08 Å shorter than In−N1, which reflects the larger trans influence of the alkoxide ligand compared to pyridine. All the In−N(py) distances in **8** [2.296(2)−2.379(2) Å], however, fall within the range of previously observed distances found in $In(NPh_2)_3(py)$ [2.264(4) Å],[13] $In(S\text{-}t\text{-}Bu)_3(py)$ [2.311(2) Å],[24] $In(SPh)_3(py)_2$ [2.374(8)−2.408(7) Å],[25] $InX_3(py)_3$ where X = Cl or Br [2.28(3)−2.38(2) Å],[26,27] and $InCl_2$(1,3-diphenyltriazenido)(3,5-dimethylpyridine)$_2$ [average 2.307(7) Å].[28] The In−N distances to the alkylamines in five-coordinate **4** and **9** [2.308(3) and 2.253(11) Å, respectively] are within the range of distances reported for $Me_3In(H_2N\text{-}t\text{-}Bu)$ [2.363(8) Å],[29] $Me_2InI(H_2N\text{-}t\text{-}Bu)$ [2.292(5) Å],[30] $MeInCl_2$-

(17) Bradley, D. C.; Chudzynska, H.; Frigo, D. M.; Hursthouse, M. B.; Mazid, M. A. *J. Chem. Soc., Chem. Commun.* **1988**, 1258.
(18) Bradley, D. C.; Chudzynska, H.; Frigo, D. M.; Hammond, M. E.; Hursthouse, M. B.; Mazid, M. A. *Polyhedron* **1990**, *9*, 719.
(19) Trentler, T. J.; Goel, S. C.; Hickman, K. M.; Viano, A. M.; Chiang, M. Y.; Beatty, A. M.; Gibbons, P. C.; Buhro, W. E. *J. Am. Chem. Soc.* **1997**, *119*, 2172.
(20) Bradley, D. C.; Frigo, D. M.; Hursthouse, M. B.; Hussain, B. *Organometallics* **1988**, *7*, 1112.
(21) Self, M. F.; McPhail, A. T.; Wells, R. L. *J. Coord. Chem.* **1993**, *29*, 27.
(22) Dembowski, U.; Pape, T.; Herbst-Irmer, R.; Pohl, E.; Roesky, H. W.; Sheldrick, G. M. *Acta Crystallogr., Sect. C* **1993**, *C49*, 1309.
(23) Rose, D. J.; Chang, Y. D.; Chen, Q.; Kettler, P. B.; Zubieta, J. *Inorg. Chem.* **1995**, *34*, 3973.
(24) Suh, S.; Hoffman, D. M. *Inorg. Chem.* **1998**, *37*, 5823.
(25) Annan, T. A.; Kumar, R.; Mabrouk, H. E.; Tuck, D. G.; Chadha, R. K. *Polyhedron* **1989**, *8*, 865.
(26) Jeffs, S. E.; Small, R. W. H.; Worrall, I. J. *Acta Crystallogr., Sect. C* **1984**, *C40*, 1329.
(27) Small, R. W. H.; Worrall, I. J. *Acta Crystallogr., Sect. C* **1982**, *C38*, 932.
(28) Leman, J. T.; Roman, H. A.; Barron, A. R. *J. Chem. Soc., Dalton Trans.* **1992**, 2183.
(29) Atwood, D. A.; Jones, R. A.; Cowley, A. H.; Bott, S. G.; Atwood, J. L. *J. Organomet. Chem.* **1992**, *434*, 143.
(30) Atwood, D. A.; Cowley, A. H.; Jones, R. A.; Atwood, J. L.; Bott, S. G. *J. Coord. Chem.* **1992**, *26*, 293.

(H_2N-*t*-Bu) [2.209(5) Å],[31] ($Me_3In)_2$(NHMe$(CH_2)_2$NHMe) [2.369(7) and 2.393(7) Å][32] and $InBr_3(H_2NSiMe_3)$ [2.210(9) Å].[33] The In−N distance in **5** [2.2004(19) Å] involving Htmp is short compared to the aforementioned distances and also much shorter than in Me_3In(Htmp) [2.502(5) Å].[32] In the latter compound, the long In−N distance was proposed to be a consequence of steric interactions between the methyl groups on indium and the methyl substituents on the amine.

Conclusion

Fluoroalkoxide complexes of indium are prepared by reacting indium tris(amide) complexes with alcohols. In[N-*t*-Bu$(SiMe_3)$]$_3$ reacts with $(CF_3)Me_2COH$ ($pK_a \approx 14-15$) to yield the homoleptic alkoxide [In{μ-$OCMe_2(CF_3)$}{$OCMe_2(CF_3)$}$_2$]$_2$, while the more acidic alcohols $(CF_3)_2MeCOH$ and $(CF_3)_2CHOH$ (pK_a = 9.6 and 9.3)[34] give In[$OCMe(CF_3)_2$]$_3$(H_2N-*t*-Bu), In[$OCH(CF_3)_2$]$_3$(H_2N-*t*-Bu)$_3$, and square-pyramidal [H_3N-*t*-Bu][In{$OCH(CF_3)_2$}$_4$(H_2N-*t*-Bu)]. It is proposed that the source of *t*-BuNH_2 in the reactions with acidic reagents is an [H_2N-*t*-Bu$(SiMe_3)$]X intermediate from which the amine is released as a leaving group upon nucleophilic attack at silicon.

The reactions of $(CF_3)_2MeCOH$ and $(CF_3)_2CHOH$ with In(tmp)$_3$ and In$(NEt_2)_3$ are simpler than those involving In[N-*t*-Bu$(SiMe_3)$]$_3$ because there is no possibility of amide breakdown. In(tmp)$_3$ reacts with 3 equiv of $(CF_3)_2CHOH$ to give In[$OCH(CF_3)_2$]$_3$(Htmp) and with 4 equiv of $(CF_3)_2$MeCOH to yield [H_2tmp][In{$OCR(CF_3)_2$}$_4$] (R = H or Me). In[$OCH(CF_3)_2$]$_3$(Htmp) can be converted quantitatively to [H_2tmp][In{$OCH(CF_3)_2$}$_4$] by the addition of alcohol. In$(NEt_2)_3$ reacts with $(CF_3)_2CHOH$ to give tbp [H_2NEt_2][In{$OCH(CF_3)_2$}$_4$($HNEt_2$)] and with $(CF_3)_2MeCOH$, followed by addition of pyridine, to yield *mer*-In[$OCMe(CF_3)_2$]$_3$(py)$_3$. These reactions of In(tmp)$_3$ and In$(NEt_2)_3$ are similar to those of In[N-*t*-Bu$(SiMe_3)$]$_3$ in that the released amines Htmp and $HNEt_2$ complicate the chemistry by forming amine adducts and/or ammonium salts via deprotonation of the acidic alcohols.

The dimer [In{μ-$OCMe_2(CF_3)$}{$OCMe_2(CF_3)$}$_2$]$_2$ is the first structurally characterized example of an indium(III) tris(alkoxide) complex. We prepared these indium fluoroalkoxide complexes with the intent of using one or more of them as precursors to fluorine-doped indium oxide films. Among the new compounds, In[$OCMe(CF_3)_2$]$_3$(H_2N-*t*-Bu) is an attractive precursor candidate because of its high volatility and ease of preparation. Chemical vapor deposition studies using In[$OCMe(CF_3)_2$]$_3$(H_2N-*t*-Bu) as a precursor are in progress.

Acknowledgment for technical assistance with the crystal structure determinations is made to Dr. James Korp. This work was supported in part by the Robert A. Welch Foundation, by the MRSEC Program of the National Science Foundation under Award No. DMR-9632667, and by the State of Texas through the Texas Center for Superconductivity at the University of Houston and the Advanced Research Program.

Supporting Information Available: X-ray crystallographic files, in CIF format, for compounds **1**, **4**, **5**, **7**, and **8** are available free of charge via the Internet at http://pubs.acs.org. The X-ray crystallographic file for **9** is available from the authors.

IC990315J

(31) Veith, M.; Recktenwald, O. *J. Organomet. Chem.* **1984**, *264*, 19.
(32) Bradley, D. C.; Dawes, H.; Frigo, D. M.; Hursthouse, M. B.; Hussain, B. *J. Organomet. Chem.* **1987**, *325*, 55.
(33) Kühner, S.; Hausen, H.-D.; Weidlein, J. *Z. Anorg. Allg. Chem.* **1998**, *624*, 13.
(34) Willis, C. J. *Coord. Chem. Rev.* **1988**, *88*, 133.